Finite-Difference Approach to the Solution of Time-Domain Integral Equations for Layered Structures

Natalia Georgieva, *Student Member, IEEE,* and Eikichi Yamashita, *Fellow, IEEE*

***Abstract*—A numerical algorithm for the analysis of transient electromagnetic fields in planar structures is proposed based on the time-domain magnetic-field integral equation (MFIE), electric-field integral equation (EFIE), and the marching-on-in-time approach. The field vectors are represented in terms of vector potential functions which are calculated either by integration or by the three-dimensional (3-D) wave equation according to the geometry of the structure. Thus, the algorithm combines the advantages of integral equation techniques and finite-difference schemes. While this approach is applicable to any geometries, it is especially suitable for multilayered planar structures and is competitive to the finite-difference time-domain (FDTD) method in the case of open and radiating problems. Theoretical results are verified by the analysis of a pulse propagation in a homogeneous open-end microstrip line.**

***Index Terms*—Integral-equation method, time-domain analysis.**

I. Introduction

SINCE the finite-difference time-domain (FDTD) approach has been introduced for wide application to transient electromagnetic fields, the interest in time-domain integral-equation (TDIE) approaches faded considerably. There were good reasons for this—high requirements in respect to central processing unit (CPU) time (integration is much more time consuming than differentiation), problems with the analysis of infinitesimally thin plates where the magnetic-field integral equation (MFIE) is unsuitable [7] and the electric-field integral equation (EFIE) displays instabilities at later time-steps. In addition, the implementation of the TDIE was entirely restricted to scattering (open) problems.

On the other hand, the main advantage of the TDIE, i.e., easy treatment of open structures, and reduction of a three-dimensional (3-D) problem to a two-dimensional (2-D) one, remains important and attractive for many implementations. Despite the intensive research for numerical approximations of radiation/transmission conditions for finite-difference schemes, there are still problems with their implementation to open problems. Publications recently appeared which show successful attempts to combine the advantages of finite-difference techniques with the integral-equation approach [8], [11]. While [11] combines the FDTD method with the integral equation technique for remote objects, [8] is entirely based on the TDIE, yet applies a finite-difference approach for their solution. This approach is known to reduce the singularity of the kernel of the evaluated integrals which now appear to be exactly the vector potential functions (see R. Mittra, [2]).

A similar approach has been applied in the present method which shows a further possibility to reduce the CPU time and memory requirements of the TDIE by calculation of the vector potential functions by the 3-D wave equation, and to improve the overall stability by the displacement of the equivalent magnetic and electric currents by a half-step in space and by a half-step in time. It presents a new possibility for the implementation of the TDIE to the analysis of transient fields in transmission-line problems and scattering from planar structures. It is equally suited to open and closed problems but is advantageous in comparison with the FDTD if radiating boundaries are present. The approach is based on the surface MFIE and EFIE, thus, reducing the 3-D problem to a 2-D one. At every surface point, only four tangential field components are calculated. It is shown that infinite planes can also be treated by reducing them to finite numerical planes. The outer-to-numerical plane integration is substituted by a contour integration of the artificial contour boundary of the numerical plane. The vector potential functions of self-planes has been calculated by the 3-D wave equation, which improves the overall speed of the algorithm.

II. Theory

A. Time-Domain Integral Equations

The conventional form of the TDIE is [1] as shown in (1) and (2) at the bottom of the next page, where: Θ is the solid angle which opens from the point of observation P to the surface of the analyzed volume; R is the distance between P and the point of integration Q; $\hat{r}$ is the unit vector of R (from Q to P); $\hat{n}$ is the inward normal of the integrated surface; $\tau = t - R/v$ is the retarded time; $\vec{J}^i$,$\vec{K}^i$ is the induced electric and magnetic currents; ρ, m are the electric and magnetic charges; and the L operator is $L\{f\} = \frac{f}{R^2} + \frac{1}{vR}\frac{\partial f}{\partial \tau}$.

In the following approach, the EFIE and MFIE are viewed in a somewhat different way, i.e. the fields are expressed via the vector potentials

$$\vec{A}_{(P,t)} = \frac{\mu}{4\pi}\left[\int_v \frac{\vec{J}^i(Q,\tau)}{R}dv_Q + \oint_s \frac{\hat{n}\times\vec{H}(Q,\tau)}{R}ds_Q\right] \quad (3)$$

Manuscript received January 22, 1997; revised February 28, 1997.

The authors are with the Department of Electronic Engineering, University of Electro-Communications, Chofu-shi, Tokyo 182, Japan.

Publisher Item Identifier S 0018-9480(97)03923-9.

$$\vec{F}_{(P,t)} = \frac{\varepsilon}{4\pi}\left[\int_v \frac{\vec{K}^i(Q,\tau)}{R}dv_Q + \oint_s \frac{\vec{E}(Q,\tau)\times\hat{n}}{R}ds_Q\right] \quad (4)$$

so that the superposition of the fields created by both electric and magnetic sources yields

$$\vec{H} = -\frac{\partial\vec{F}}{\partial t} - \nabla\psi + \frac{1}{\mu}\nabla\times\vec{A} \quad (5)$$

$$\vec{E} = -\frac{\partial\vec{A}}{\partial t} - \nabla\varphi - \frac{1}{\varepsilon}\nabla\times\vec{F}. \quad (6)$$

Here, φ and ψ are scalar potential functions related to the vector potentials via the Lorentz gauge condition

$$\frac{\partial\varphi}{\partial t} = -v^2\nabla.\vec{A} \quad (7)$$

$$\frac{\partial\psi}{\partial t} = -v^2\nabla.\vec{F}. \quad (8)$$

Now the TDIE can be written as

$$\Theta\frac{\partial\vec{H}}{\partial t} = -\varepsilon\frac{\partial^2}{\partial t^2}(\vec{I}_F) + \frac{1}{\mu}\nabla\nabla.\vec{I}_F + \frac{\partial}{\partial t}\nabla\times\vec{I}_A \quad (9)$$

$$\Theta\frac{\partial\vec{E}}{\partial t} = -\mu\frac{\partial^2}{\partial t^2}(\vec{I}_A) + \frac{1}{\varepsilon}\nabla\nabla.\vec{I}_A - \frac{\partial}{\partial t}\nabla\times\vec{I}_F \quad (10)$$

where $\vec{I}_A = \frac{4\pi}{\mu}\vec{A}$; $\vec{I}_F = \frac{4\pi}{\varepsilon}\vec{F}$.

From a theoretical point of view, both sets of equations (1), (2) and (9), (10), are equivalent; however, from a numerical point of view there are substantial differences: 1) in the type of integrals involved; 2) in the possibility for application of a time-space leap-frog scheme to ensure stability of the time-marching solution; and 3) in the complete elimination of normal–to–surface field components. The space operators $\nabla\nabla.$ and $\nabla\times$ are easy to implement for plane surfaces. In this case also, $\Theta = 2\pi$. After introducing equivalent surface currents according to the surface relations

$$\hat{n}\times\vec{H} = \vec{J} \quad (11)$$

$$\hat{n}\times\vec{E} = -\vec{K} \quad (12)$$

and a limiting procedure for the observation point approaching the boundary ([1], [5]) the following equations are obtained:

$$2\pi\frac{\partial\vec{K}}{\partial t} = \hat{n}\times\left[\mu\frac{\partial^2}{\partial t^2}(\vec{I}_A) - \frac{1}{\varepsilon}\nabla_s\nabla_s.\vec{I}_A + \frac{\partial}{\partial t}\nabla\times\vec{I}_F\right] \quad (13)$$

$$2\pi\frac{\partial\vec{J}}{\partial t} = \hat{n}\times\left[-\varepsilon\frac{\partial^2}{\partial t^2}(\vec{I}_F) + \frac{1}{\mu}\nabla_s\nabla_s.\vec{I}_F + \frac{\partial}{\partial t}\nabla\times\vec{I}_A\right]. \quad (14)$$

The singularity of the tangential fields at an observation point lying on the surface results in the coefficient (2π) and is a consequence of the third member of (13), (14), since [3]

$$\nabla\times\int_s\frac{\vec{J}}{R}ds = \oint_s\nabla\times\left[\frac{\vec{J}}{R}\right]ds - 2\pi[\hat{n}\times\vec{J}].$$

The above equations are applied to describe the fields at the boundary of each region characterized by its parameters ε and μ. At the common interface, they are coupled by the boundary conditions for their equivalent currents

$$\vec{K}^{(1)} = -\vec{K}^{(2)} \quad (15)$$

$$\vec{J}^{(1)} = -\vec{J}^{(2)}. \quad (16)$$

In the case of a conducting surface, $\vec{K}^{(1)} = \vec{K}^{(2)} = 0$, and the equivalent electric currents, $\vec{J}^{(1)}$ and $\vec{J}^{(2)}$, which are now actual currents, are decoupled.

The equations for points at the interface of neighboring regions are obtained by a linear combination of the equations for both regions and by using the above boundary conditions (15) and (16):

a) region 1:

$$2\pi\frac{\partial\vec{K}^{(1)}}{\partial t} = \hat{n}_1\times\left[\mu_1\frac{\partial^2}{\partial t^2}(\vec{I}_A^{(1)}) - \frac{1}{\varepsilon_1}\nabla_s\nabla_s.\vec{I}_A^{(1)} + \frac{\partial}{\partial t}\nabla\times\vec{I}_F^{(1)}\right] \quad (17)$$

$$2\pi\frac{\partial\vec{J}^{(1)}}{\partial t} = \hat{n}_1\times\left[-\varepsilon_1\frac{\partial^2}{\partial t^2}(\vec{I}_F^{(1)}) + \frac{1}{\mu_1}\nabla_s\nabla_s.\vec{I}_F^{(1)} + \frac{\partial}{\partial t}\nabla\times\vec{I}_A^{(1)}\right] \quad (18)$$

b) region 2:

$$2\pi\frac{\partial\vec{K}^{(1)}}{\partial t} = \hat{n}_1\times\left[\mu_2\frac{\partial^2}{\partial t^2}(\vec{I}_A^{(2)}) - \frac{1}{\varepsilon_2}\nabla_s\nabla_s.\vec{I}_A^{(2)} + \frac{\partial}{\partial t}\nabla\times\vec{I}_F^{(2)}\right] \quad (19)$$

$$2\pi\frac{\partial\vec{J}^{(1)}}{\partial t} = \hat{n}_1\times\left[-\varepsilon_2\frac{\partial^2}{\partial t^2}(\vec{I}_F^{(2)}) + \frac{1}{\mu_2}\nabla_s\nabla_s.\vec{I}_F^{(2)} + \frac{\partial}{\partial t}\nabla\times\vec{I}_A^{(2)}\right]. \quad (20)$$

Equation (17) is multiplied by α and is added to (19). Similarly, (18) is multiplied by β and is added to (20). The

---

$$\Theta\vec{H}(P,t) = \int_v\left(-\varepsilon\frac{1}{R}\frac{\partial\vec{K}^i}{\partial\tau} + L\{\vec{J}^i\times\hat{r} + \frac{1}{\mu}m.\hat{r}\}\right)dv_Q + \oint_s\left(\varepsilon\frac{1}{R}\frac{\partial}{\partial\tau}[\hat{n}\times\vec{E}] + L\{[\hat{n}\times\vec{H}]\times\hat{r} + [\hat{n}.\vec{H}].\hat{r}\}\right)ds_Q \quad (1)$$

$$\Theta\vec{E}(P,t) = \int_v\left(-\mu\frac{1}{R}\frac{\partial\vec{J}^i}{\partial\tau} + L\{-\vec{K}^i\times\hat{r} + \frac{1}{\varepsilon}\rho.\hat{r}\}\right)dv_Q + \oint_s\left(-\mu\frac{1}{R}\frac{\partial}{\partial\tau}[\hat{n}\times\vec{H}] + L\{[\hat{n}\times\vec{E}]\times\hat{r} + [\hat{n}.\vec{E}].\hat{r}\}\right)ds_Q \quad (2)$$

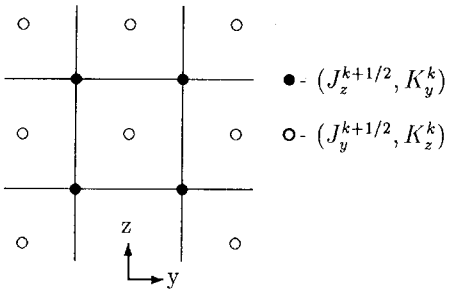

Fig. 1. Open microstrip line.

right choice of coefficients when combining both regions' equations is discussed in detail in [6]. To obtain a unique solution, α and β must satisfy the relation ($\alpha\beta$), which is positive and real. They should also ensure that the coefficients of the second-derivative-in-time terms become the same. This is essential for the time-stepping procedure where the self-patch terms in the right-hand side (RHS) should vanish, thus providing decoupling of the equations for the $\vec{J}$ and $\vec{K}$ currents and elimination of the forward-in-time values. Therefore, $\alpha = \mu_{r_2}/\mu_{r_1}$ and $\beta = \varepsilon_{r_2}/\varepsilon_{r_1}$. In the considered example of an open microstrip structure, region (1) is the dielectric substrate with the dielectric constant ε_{r_1} and region (2) is the air region with $\varepsilon_{r_2} = 1$ (see Fig. 1). For both regions, $\mu_r = 1$. This linear combination finally yields the following equations for observation points at the dielectric interface:

$$4\pi\frac{\partial\vec{K}^1}{\partial t} = \hat{n}_1 \times \left[\mu_0\frac{\partial^2}{\partial t^2}\left(\vec{I}_A^1 + \vec{I}_A^2\right) - \frac{1}{\varepsilon_0}\nabla_s\nabla_s.\left(\frac{1}{\varepsilon_{r_1}}\vec{I}_A^1 + \vec{I}_A^2\right) + \frac{\partial}{\partial t}\nabla\times\left(\vec{I}_F^1 + \vec{I}_F^2\right)\right] \tag{21}$$

$$2\pi\left(1+\frac{1}{\varepsilon_{r_1}}\right)\frac{\partial\vec{J}^1}{\partial t} = \hat{n}_1 \times \left[-\varepsilon_0\frac{\partial^2}{\partial t^2}\left(\vec{I}_F^1 + \vec{I}_F^2\right) + \frac{1}{\mu_0}\nabla_s\nabla_s.\left(\frac{1}{\varepsilon_{r_1}}\vec{I}_F^1 + \vec{I}_F^2\right) + \frac{\partial}{\partial t}\nabla\times\left(\frac{1}{\varepsilon_{r_1}}\vec{I}_A^1 + \vec{I}_A^2\right)\right] \tag{22}$$

where $\vec{I}_A^1$, $\vec{I}_F^1$ are the potentials calculated at retarded time $\tau_1 = t - R/v_1$. Here, $v_1 = c/\sqrt{\varepsilon_{r_1}}$ is the velocity of light in the dielectric $\vec{I}_A^2$ and $\vec{I}_A^2$ are the potentials calculated at retarded time $\tau_2 = t - R/c$. The equivalent currents in the above potential functions also satisfy the boundary conditions (15), (16). It is now obvious that the self-patch integrals in the second-derivative-in-time terms will cancel one another due to the opposite signs of the equivalent currents of both regions at the interface.

The $\vec{J}$ currents at conducting surfaces are calculated by the MFIE (14) of the respective region. It is important to note that the calculation of $\vec{J}$ currents at conducting surfaces by the separate MFIE of each region, which strongly depend on the $\vec{I}_F$ vector functions of the respective plane, ensures correct calculation even in the case of infinitesimally thin plates. This is shown in the presented simulations.

B. The Artificial Contour Boundary

The problem of the artificial contour boundary which arises in infinite cases along the y and z axes planes are now considered. The planes of interest must be limited to finite numerical planes by the artificial contour boundary. These contours must be sufficiently far away from the source plane and any discontinuities of the structure. The field components outside the contour boundary for the radiation condition [4] can then be imposed

$$\vec{E} - Z_w\vec{H}\times\hat{r} = O(R^{-2}) \tag{23}$$

$$\vec{H} - \frac{1}{Z_w}\hat{r}\times\vec{E} = O(R^{-2}) \tag{24}$$

where R is the distance from a reference point (center of the source plane) and $\hat{r}$ is the unit vector of R. From the above equations, the following radiation conditions for the equivalent surface currents are obtained:

$$\nabla_s.\vec{J} = -\frac{1}{v}\frac{\partial\vec{J}}{\partial t}\hat{r} \tag{25}$$

$$\nabla_s.\vec{K} = -\frac{1}{v}\frac{\partial\vec{K}}{\partial t}\hat{r} \tag{26}$$

which is an expected result since the $\vec{J}$ and $\vec{K}$ currents satisfying the radiation condition are $f(t - R/v)$ functions of time. Currents satisfying the above conditions are substituted in (13) and (14). After some vector manipulations it can be shown that in the contribution of the outer region currents, all terms cancel except the integrals

$$\frac{\partial\vec{K}^{ou}}{\partial t} = \frac{\mu}{2\pi}v^2\hat{n}\times\left[\nabla_P\int_s\nabla_Q.\left(\frac{\vec{J}_{ou}}{R}\right)ds + \int_s\nabla_Q\left(\frac{\nabla_Q.\vec{J}_{ou}}{R}\right)ds\right] \tag{27}$$

where $\vec{K}^{ou}$ denotes the contribution to the internal $\vec{K}$ of the external-to-numerical region currents $\vec{J}_{ou}$. The equation for the $\vec{J}^{ou}$ time derivative is dual. Obviously the above surface integrals reduce to contour integrals

$$\frac{\partial\vec{K}^{ou}}{\partial t} = \frac{\mu}{2\pi}v^2\hat{n}\times\left[\nabla_P\oint\frac{\vec{J}\hat{n}_c}{R}dl + \oint\frac{\nabla_Q.\vec{J}}{R}\hat{n}_c dl\right] \tag{28}$$

where $\hat{n}_c$ is the outward normal to the contour of the outer region. Thus, the outer region contribution reduces to integration of the currents at the contour artificial boundary of the numerical plane. It is then added to the contribution of the inner patches. When treating the artificial boundary at the dielectric-to-air interface, the same linear combinations of equations are applied.

C. Calculation of the Vector Potential Functions

The integral functions $\vec{A}$ and $\vec{F}$ as defined in (3) and (4) are a superposition of the potentials created by all (equivalent and actual) sources as if radiating in free space with the respective dielectric and magnetic constants. There are two ways of calculating the contribution of every surface plane as cited below.

1) Direct Integration: Currents are assumed constant at every patch. Therefore, an integral of the type

$$I_r = \iint_{-1/2}^{1/2} \frac{1}{\sqrt{(\xi+\Delta n_i)^2+(\eta+\Delta n_j)^2+\Delta n_k^2}}\, d\xi d\eta$$

has to be calculated. Here, $\Delta n_i, \Delta n_j, \Delta n_k$ denote the number of space steps between the observation and integration point. This integral has an analytical solution and is quickly calculated during the time-stepping procedure. The integration approach is definitely advantageous when the potentials of remote planes are calculated. Of course, it is also applicable when the observation point lies in the plane where potential functions are calculated. However, there exists another possibility which produces the same results with less computation time, as explained below.

2) Solving the 3-D Wave Equation: Both $\vec{A}$ and $\vec{F}$ are solutions of the wave equation when conditions (7), (8) are imposed

$$\triangle\vec{A} - \frac{1}{v^2}\frac{\partial^2\vec{A}}{\partial t^2} = -\mu\vec{J}_v \tag{29}$$

$$\triangle\vec{F} - \frac{1}{v^2}\frac{\partial^2\vec{F}}{\partial t^2} = -\varepsilon\vec{K}_v. \tag{30}$$

Here, $\vec{J}_v$ and $\vec{K}_v$ are volume currents and are assumed to be related to the equivalent surface currents as $\vec{J}_v = \vec{J}/\Delta h$, with $\vec{K}_v = \vec{K}/\Delta h$, Δh being the dimension of the patch. Due to the 2-D character of the excitation, the vector potential functions must be symmetrical in respect with the excitation plane. In this approach, the numerical absorbing boundary condition must be imposed in the case of open problems at outer boundaries of the 3-D numerical region.

Both approaches were simulated and it was found that five layers above the current sheet are enough to obtain the same results (the relative difference at most is 5%) when applying Liao's ABC [9] with the second approach. The wave equation is solved by an explicit scheme [12].

III. Discretization and Numerical Implementation

A. Common Algorithm

Surface currents are considered constant at every patch but second-order interpolation in time is applied to calculate their value at the given retarded time, i.e. three points in neighboring time-points are needed.

The electric currents and the magnetic currents are displaced in time by half a step which ensures correct treatment of the time derivatives. For exact evaluation of the space derivatives $\nabla_s\nabla_s.$ and $\nabla\times$, displacement in space by half a step is needed, too. The equivalent current components $(J_z^{k+1/2}, K_y^k)$ and $(J_y^{k+1/2}, K_z^k)$ are situated at points displaced by half a step along both y and z axes (Fig. 2). The components of the integrals $\vec{I}_A$, $\vec{I}_F$ are calculated at the points of the respective currents.

The time-step Δt and the space-step Δh are related to the higher speed of light in the structure c by

$$\Delta t = \frac{\Delta h}{cq} \tag{31}$$

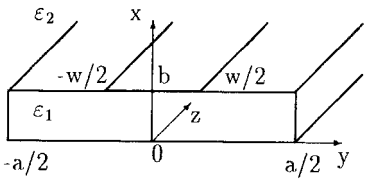

Fig. 2. Space displacement of surface currents.

where q is chosen to be $q = \sqrt{2}$, if potential functions are calculated only by integration, and $q = \sqrt{3}$, if the 3-D wave equation is solved.

Introducing the following notations:

$$\begin{aligned}
\vec{A}_\Sigma &= \vec{I}_A{}^1 + \vec{I}_A{}^2 \\
\vec{F}_\Sigma &= \vec{I}_F{}^1 + \vec{I}_F{}^2 \\
\vec{A}_\varepsilon &= \frac{1}{\varepsilon_{r_1}}\vec{I}_A{}^1 + \vec{I}_A{}^2 \\
\vec{F}_\varepsilon &= \frac{1}{\varepsilon_{r_1}}\vec{I}_F{}^1 + \vec{I}_F{}^2 \\
GD\{\vec{\xi}\} &= \Delta h^2\nabla_s\nabla_s.\vec{\xi} \\
R\{\vec{\xi}\} &= \Delta h\nabla\times\vec{\xi}
\end{aligned}$$

the following discretized equations for observation points at the dielectric interface are obtained:

$$\begin{aligned}
&\frac{4\pi}{qZ_{w_0}}(\vec{K}^k - \vec{K}^{k-1}) \\
&\quad = \hat{n}_1\times\Big[(\vec{A}_\Sigma{}^{k+1/2} - 2\vec{A}_\Sigma{}^{k-1/2} + \vec{A}_\Sigma{}^{k-3/2}) \\
&\qquad -\frac{1}{q^2}GD\{\vec{A}_\varepsilon\}^{k-1/2} \\
&\qquad +\frac{1}{qZ_{w_0}}(R\{\vec{F}_\Sigma\}^k - R\{\vec{F}_\Sigma\}^{k-1})\Big]
\end{aligned} \tag{32}$$

$$\begin{aligned}
&2\pi\frac{Z_{w_0}}{q}(1+\frac{1}{\varepsilon_{r_1}})(\vec{J}^{k+1/2} - \vec{J}^{k-1/2}) \\
&\quad = \hat{n}_1\times\Big[-(\vec{F}_\Sigma{}^{k+1} - 2\vec{F}_\Sigma{}^k + \vec{F}_\Sigma{}^{k-1}) + \frac{1}{q^2}GD\{\vec{F}_\varepsilon\}^k \\
&\qquad +\frac{Z_{w_0}}{q}(R\{\vec{A}_\varepsilon\}^{k+1/2} - R\{\vec{A}_\varepsilon\}^{k-1/2})\Big]
\end{aligned} \tag{33}$$

where $Z_{w_0} = \sqrt{\mu_0/\varepsilon_0}$.

The electric currents at the conducting surfaces are calculated by the MFIE

$$\begin{aligned}
&2\pi\frac{Z_{w_0}}{q\varepsilon_{r_i}}(\vec{J}_{c_i}^{k+1/2} - \vec{J}_{c_i}^{k-1/2}) \\
&\quad = \hat{n}_i\times\Big[-(\vec{I}_{F_i}{}^{k+1} - 2\vec{I}_{F_i}{}^k + \vec{I}_{F_i}{}^{k-1}) + \frac{1}{q^2\varepsilon_{r_i}}GD \\
&\qquad \cdot\{\vec{I}_{F_i}\}^k + \frac{Z_{w_0}}{q\varepsilon_{r_i}}(R\{\vec{I}_{A_i}\}^{k+1/2} - R\{\vec{I}_{A_i}\}^{k-1/2})\Big]
\end{aligned} \tag{34}$$

where the index i indicates the respective region $(i = 1, 2)$.

The above equations provide the algorithm for a marching-on-in-time procedure. All right-hand members include currents at previous moments of time. This refers to $\vec{A}_\Sigma{}^{k+1/2}$ and $\vec{F}_\Sigma{}^{k+1}$, too. The self-patch contribution (where retardation is zero) is simply nullified because of the opposite signs

of currents at the interface. The integrals in $\vec{I}_{F_i}{}^{k+1}$ in the equation for the surface currents at conductors also include retarded magnetic currents $\vec{K}$, which are nonzero only at the interface patches away from the conducting surfaces.

The algorithm produces only the tangential components of the surface fields, but the normal ones can be easily derived by the boundary relations

$$\frac{\partial}{\partial t}(\hat{n}\vec{H}) = \frac{1}{\mu}\nabla_s.(\hat{n}\times\vec{E}) = -\frac{1}{\mu}\nabla_s.\vec{K} \tag{35}$$

$$\frac{\partial}{\partial t}(\hat{n}\vec{E}) = -\frac{1}{\varepsilon}\nabla_s.(\hat{n}\times\vec{H}) = -\frac{1}{\varepsilon}\nabla_s.\vec{J}. \tag{36}$$

B. Excitation

Unlike scattering problems where the incident field is usually analytically calculated as a Gaussian pulse in time, in the considered case of a transmission-line problem, it is calculated numerically by integrating the source plane according to the common algorithm. The presented results were obtained by an electric currents' excitation. These currents have only x-component and the excitation sheet is situated under the strip in region 1 (see Fig. 1). Currents are considered constant at the whole sheet and are a Gaussian pulse function of time. The excitation plane is discretized in the same way as the boundaries of both regions. Obviously, the excitation of equivalent $\vec{J}$ currents comes from the $\nabla\times\vec{I}_A^i$ [see (14)]. The excitation of $\vec{K}$ currents is obtained from the $\nabla\nabla.\vec{I}_A^i$ [see (13)]. Explicitly, this term is calculated according to the relations

$$\vec{I}^i = \nabla\nabla.\int_s \frac{\vec{J}^i(Q,\tau)}{R}ds_Q.$$

If the $\nabla.$ operator is inserted under the sign of the integral one obtains [4]

$$\vec{I}^i = \nabla_P\int_s\left[-\nabla_Q.\left(\frac{\vec{J}^i}{R}\right)+\frac{(\nabla_Q.\vec{J}^i)_\tau}{R}\right]ds_Q. \tag{37}$$

The $(\nabla_Q.\vec{J}^i)_\tau$ term denoting the current's divergence at a fixed retarded time τ obviously equals zero since the currents are a constant function of space coordinates at the source plane; however, the first term is nonzero and it yields (Gauss theorem)

$$\vec{I}^i = \nabla_P\oint\left(\frac{\vec{J}^i}{R}\right).\hat{n_c}dl \tag{38}$$

where $\hat{n_c}$ denotes the inward normal of the contour bounding the source plane. Therefore, this integration is performed to correctly represent the $\vec{K}$ current's excitation.

IV. Numerical Results

Two microstrip structure simulations are presented and compared with results obtained by a FDTD algorithm with perfectly matched-layer (PML) boundary conditions. The code is written in FORTRAN 90 which provides convenient tools for matrix manipulations.

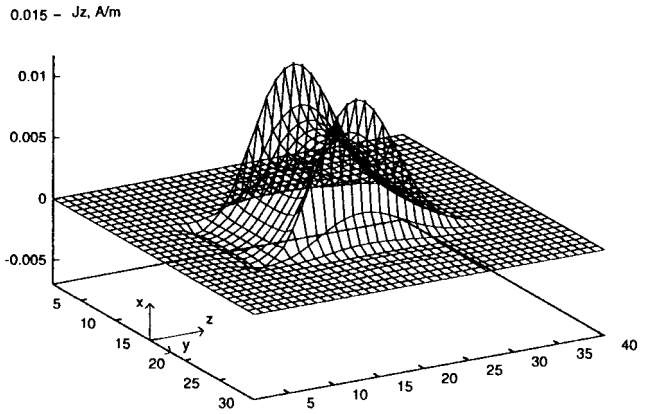

Fig. 3. Longitudinal component of electric current J_z, $t = 90\Delta t$.

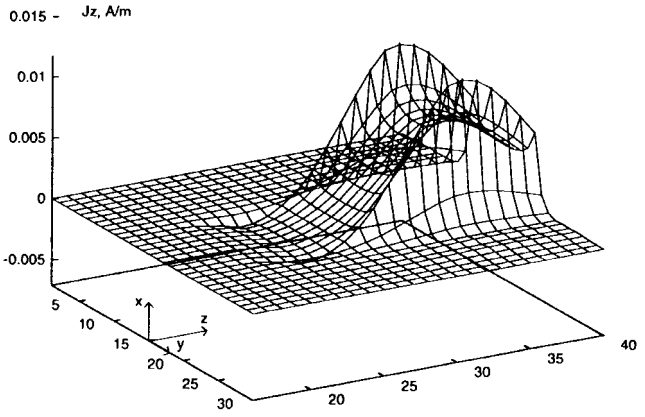

Fig. 4. Longitudinal component of electric current J_z, $t = 130\Delta t$.

1) Microstrip Line: Numerical simulation was carried out for the microstrip line in Fig. 2 with number of space steps $A = 30$ in the y-direction, $L = 40$ in the z-direction, strip width $W = 6$ and substrate thickness $B = 6$. The space-step is $\Delta h = 0.1$ mm. The dielectric constant of the substrate is $\varepsilon_r = 9$. The Gaussian pulsewidth (from maximum value to cut point) is assumed $\beta = 30$

$$G(t) = \exp\left[-\alpha(t-\beta\Delta t)^2)\right]. \tag{39}$$

The algorithm appears to be very sensitive to the choice of α, which must satisfy

$$\alpha \geq \frac{16}{(\beta\Delta t)^2}$$

which, in turn, ensures smooth excitation and truncation level of the pulse at approximately -140 dB. The amplitude of the excitation surface currents is set to $M = 1/Z_w$, where Z_w is the impedance of the dielectric region.

Fig. 3 shows the longitudinal J_z surface current (H_y component) at time-step $90\Delta t$, and Fig. 4 shows the same current at $t = 130\Delta t$. The normal H_x component was also calculated by (35), and can be seen in Fig. 5.

2) Microstrip Open End: A simple discontinuity of the above microstrip (see Fig. 6) is analyzed for a substrate with dielectric constants $\varepsilon_r = 3$. The source plane is located exactly at the middle of the line and the open end is located at $z = 14\Delta t$. Figs. 7 and 8 show the incident and reflected J_z

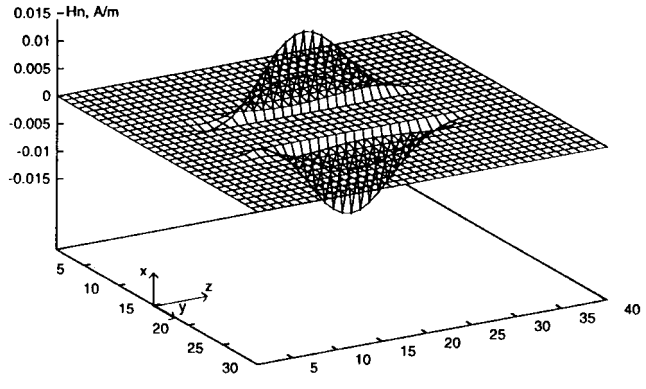

Fig. 5. Normal component of magnetic field H_x, $t = 90\Delta t$.

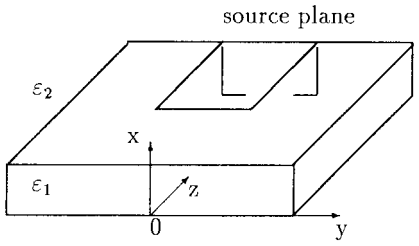

Fig. 6. Open-end microstrip line.

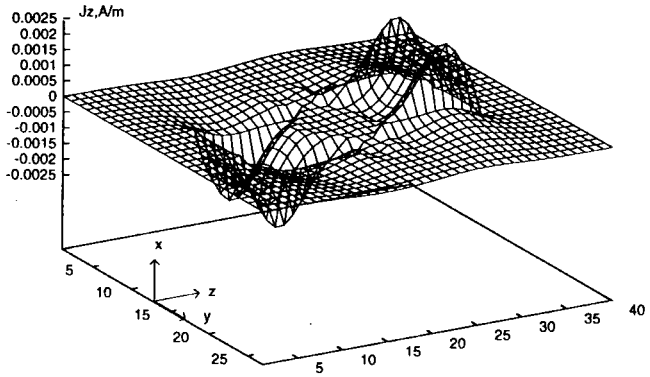

Fig. 7. J_z component, $t = 90\Delta t$.

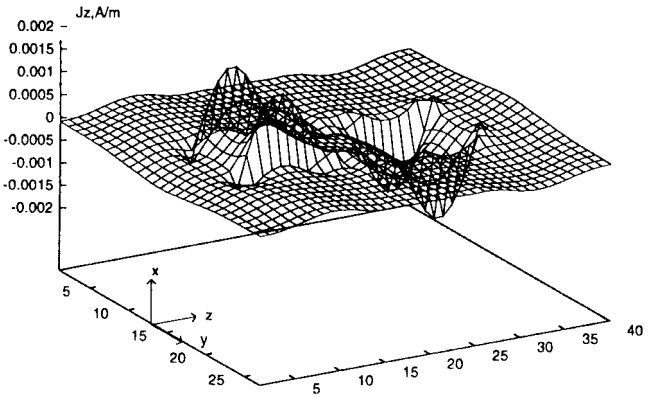

Fig. 8. J_z component, $t = 110\Delta t$.

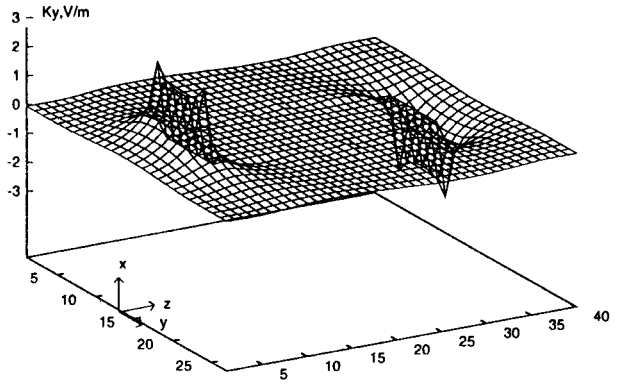

Fig. 9. K_y component, $t = 100\Delta t$.

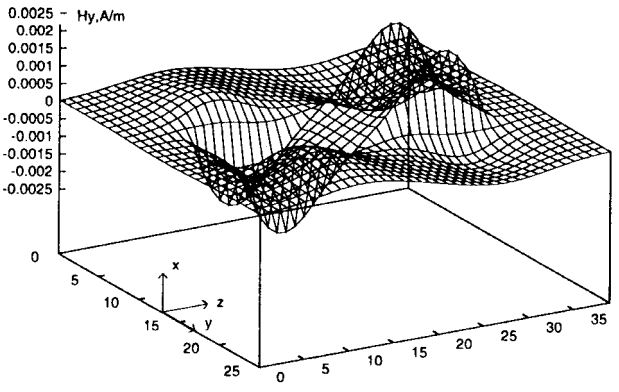

Fig. 10. H_y component, $t = 90\Delta t$, FDTD–PML.

current. Fig. 9 shows the expected singular behavior of K_y current (E_z component) at the open end. Figs. 10–12 show the results obtained by the FDTD algorithm with electric-field excitation at the same excitation plane. It must be noted that the H_y component by the FDTD algorithm is calculated a half-step above the interface (in the air) as a result of the Yee cell location at conducting planes or dielectric interfaces.

The calculation time by the proposed algorithm is mostly determined by the itegration of remote planes and for the above structure takes approximately 7 min for the pulse to be fully absorbed (350 time-steps). Memory requirements are determined by the storage of K_y, K_z, J_y, J_z values at every surface point back to a time-point determined by the largest dimension of the structure. Thus, for the above structure, the time-history package should contain

$$NT = INT\left(q\sqrt{\varepsilon_r}\sqrt{A^2 + L^2 + B^2}\right)$$

number of elements. Here, q is the constant defined in (31). Besides, at conductor planes $K_y = K_z = 0$. Therefore, the memory requirements depend: 1) on the presence of conductors; 2) on the geometry of the structure; and 3) on the dielectric constant.

V. Conclusion

A new possibility for the TDIE analysis of transient fields in layered structures is proposed in this paper. The integral equations are represented and numerically solved by a novel finite-difference approach. A technique for coupling the integral equations on mixed conductor and dielectric interfaces has been developed. It has been proven that infinite planes can be

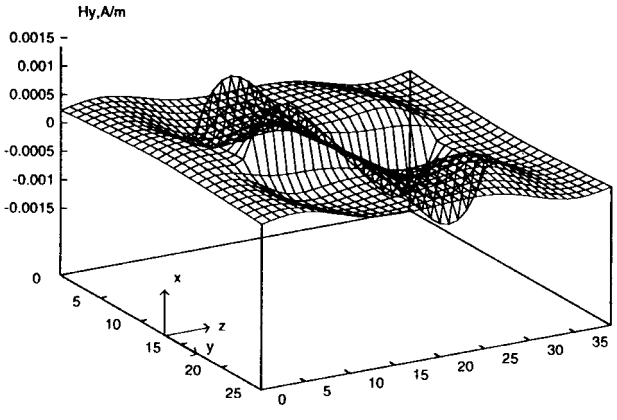

Fig. 11. H_y component, $t = 110\Delta t$, FDTD–PML.

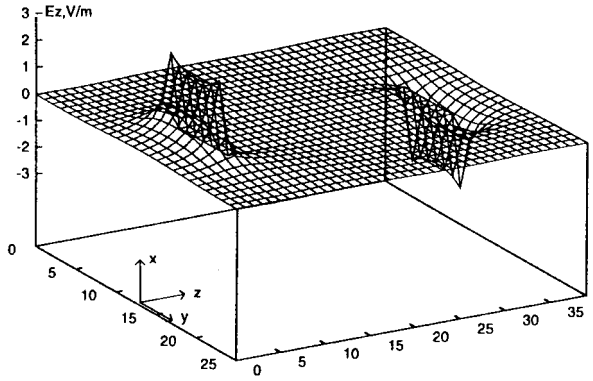

Fig. 12. E_z component, $t = 100\Delta t$, FDTD–PML.

treated by imposing the radiation condition for the equivalent currents in the region outer to the finite numerical plane. It has further been shown that the method is especially suitable for radiating and open boundary problems.

ACKNOWLEDGMENT

The authors would like to thank S. Saario for the simulations which he carried out with his FDTD-PML program and for the helpful discussions concerning comparisons between FDTD and the TDIE techniques. They are also grateful to Prof. Kishi and Dr. Qian for their support and advice during the theoretical development of the method.

REFERENCES

[1] R. Mittra, Ed., *Computer Techniques for Electromagnetics*. New York: Pergamon, 1973.
[2] L. B. Felsen, Ed., *Transient Electromagnetic Fields*. Berlin, Germany: Springer-Verlag, 1976.
[3] D. Colton and R. Kress, *Integral Equation Methods in Scattering Theory*. New York: Wiley, 1983.
[4] D. S. Jones, *Methods in Electromagnetic Wave Propagation*. Oxford, U.K.: Clarendon Press, 1994.
[5] N. Morita, N. Kumagai, and J. Mautz, *Integral Equation Methods for Electromagnetics*. Norwood, MA: Artech House, 1990.
[6] H. Mieras and C. L. Bennett, "Space-time integral equation approach to dielectric targets," *IEEE Trans. Antennas Propagat.*, vol. AP-30, pp. 2–9, Jan. 1982.
[7] R. Mittra, Y. Rahmat-Samii, D. V. Jamnejad, and W. A. Davis, "A new look at the thin-plate scattering problem," *Radio Sci*., vol. 8, no. 10, pp. 869–875, Oct. 1973.
[8] D. A. Vechinski, S. M. Rao, and T. K. Sarkar, "Transient scattering from three-dimensional arbitrarily shaped dielectric bodies," *J. Opt. Soc. Amer., A Opt. Image Sci.*, vol. 11, no. 4, pp. 1458–1470, Apr. 1994.
[9] Z. P. Liao , "A transmitting boundary for transient wave analyzes," *Scientia Sinica (Series A)*, vol. XXVII, no. 10, pp. 1063–1075, Oct 1984.
[10] E. Marx, "Integral equation for scattering by a dielectric," *IEEE Trans. Antennas Propagat.*, vol. AP-32, no. 2, pp. 166–172, Feb. 1984.
[11] J. M. Johnson and Y. Rahmat-Samii, "Multiple region FDTD (MR/FDTD) and its application to microwave analysis and modeling," in *Proc. IEEE MTT-S Symp. Dig.*, San Francisco, CA, June 1996, pp. 1475–1479.
[12] J. C. Strikwerda, *Finite Difference Schemes and Partial Differential Equations*, (Cole Mathematics Series). Pacific Grove, CA: Wadsworth & Brooks/Cole, 1989.

Natalia Georgieva (S'93) received the Dipl. Eng. (electronics) from the Technical University of Varna, Bulgaria, in 1989, and is currently working toward the Doctor (Eng.) degree at the University of Electro-Communications, Tokyo, Japan.

Her research interests include time-domain techniques in electromagnetics and their numerical implementation to the analysis of passive structures.

Eikichi Yamashita (M'66–SM'79–F'84) was born in Tokyo, Japan, on February 4, 1933. He received the B.S. degree from the University of Electro-Communications, Tokyo, Japan, and the M.S. and Ph.D. degree from the University of Illinois, Urbana, all in electrical engineering, in 1956, 1963, and 1966, respectively.

From 1956 to 1964, he was a member of the research staff on millimiter-wave engineering at the Electrotechnical Laboratory. While on leave (1961–1963, 1964–1966), he studied solid-state devices in the millimeter-wave region at the Electro-Physics Laboratory, University of Illinois, Urbana. In 1967, he became an Associate Professor in the Department of Electronic Engineering, University of Electro-Communications, a Professor in 1977, and from 1992 to 1994, Dean of the Graduate School. He was editor of *Analysis Methods for Electromagnetic Wave Problems* (vols. I and II, Artech House). His research since 1956 has been principally on applications of electromagnetic waves, such as various microstrip transmission lines, wave propagation in gaseous plasma, pyroelectric-effect detectors in the submillimiter-wave region, tunnel-diode oscillators, wide-band laser modulators, various types of optical fibers, ultra-short electrical pulse propagation on transmission lines, and millimiter-wave imaging.

Dr. Yamashita was chairperson of the Technical Group on Microwaves, IEICE, Japan, from 1985 to 1986, and vice-chairperson, Steering Committee, Electronics Group, IEICE, from 1989 to 1990. He served as associate editor of the IEEE TRANSACTIONS ON MICROWAVE THEORY AND TECHNIQUES from 1980 to 1984, and again in 1996. He was elected chairperson of the IEEE MTT-S Tokyo Chapter from 1985 to 1986. He has been a member of the IEEE MTT-S ADCOM since January 1992, and chairperson of Chapter Operations Committee, IEEE Tokyo Section, since 1995. In 1990 and 1994, he served as chairperson of International Steering Committee, Asia–Pacific Microwave Conference, held in Tokyo and sponsored by the IEICE.